

# Highly ordered in-plane orientation of single-walled carbon nanotubes

LU JIA<sup>a,b</sup>, YAFEI ZHANG<sup>b\*</sup>, JINYONG LI<sup>b</sup>, CHANG YOU<sup>b</sup>, ERQING XIE<sup>a</sup>

<sup>a</sup>*Institute of Electronic Materials, School of Physics, Lanzhou University, Lanzhou 730000, PR China*

<sup>b</sup>*Research Institute of Micro/Nanometer Science and Technology, Shanghai Jiao Tong University, Shanghai 200240, PR China*

Single-walled carbon nanotubes (SWNTs) were functionalized with amphiphilic octadecylamine (ODA), and the solubility of SWNTs in chloroform was largely enhanced. The surface pressure-area isotherm indicated good spreading properties of functionalized SWNTs. According to scanning electron microscopy (SEM) images, highly ordered in-plane orientation of SWNT films was achieved by Langmuir–Blodgett (LB) technique at room temperature. The distance between the aligned SWNTs decreased with increasing surface pressure. Homogeneous multilayers were obtained via layer-by-layer deposition. The current-voltage (I-V) characteristics of multilayer films were investigated, in which the SWNTs were aligned perpendicularly and parallel to the electrodes, respectively.

(Received March 12, 2008; accepted August 14, 2008)

*Keywords:* Single-walled carbon nanotube; Langmuir–Blodgett film; SEM; Current-voltage curve

## 1. Introduction

Due to their exceptional electrical, mechanical, and thermal properties [1-4], one-dimension (1-D) material single-walled carbon nanotubes (SWNTs) have drawn great interest of many researchers, and have been widely investigated in the fields such as electron field emitters [5], quantum wires [6], molecular filters [7], hydrogen storage [8], flat panel displays [9] and field effect transistors (FET) [10]. SWNTs are normally produced by arc-discharge [4], chemical vapor deposition (CVD) [11, 12], high-pressure CO gas decomposition (HiPCO) [13], or laser ablation (LA) [14], all of which generally lead to randomly oriented nanotubes. Thus, in order to organize the SWNTs into functional assemblies and working systems, preparing homogeneous thin film of aligned SWNTs is a big challenge to be confronted. So far, aligned SWNTs have been obtained by means of electrophoresis [15, 16], magnetic alignment [17], nanotemplate [18], electrospinning technique [19], and gas flow [20]. However, it is still difficult to obtain highly ordered, large-scale, uniform and controllable films of in-plane aligned SWNTs under room temperature. Langmuir–Blodgett (LB) technique is employed to prepare aligned SWNT films which has the following appealing characteristics: large-area and highly ordered films can be formed; the silicon and other substrates can be used around room temperature; the inter-particle distance and the final superstructures can be finely controlled; and multiple or alternating layer is also fairly easy and quite efficient to be carried out. Up to now, research on the SWNT LB films and the electronic properties is very limited, to our understanding.

In this paper, purified SWNTs were functionalized with amphiphilic octadecylamine (ODA). Fourier Transform Infrared spectra (FTIR) were performed on the

functionalized SWNTs. The solubility of the chemically modified SWNTs was investigated. The tubes were aligned by LB technique at room temperature. The scanning electron microscopy (SEM) images of monolayer under different surface pressures were analyzed. The current-voltage (I-V) curves of multilayers were recorded, in which SWNTs were deposited perpendicularly or parallel to the electrodes.

## 2. Experimental

Arc-discharge synthesized SWNTs with typical length of 1~3  $\mu\text{m}$  and average diameter of 1.4 nm were used. Standard purification and cutting process were taken [21]. The purified SWNTs were refluxed in thionyl chloride ( $\text{SOCl}_2$ ) for 24 hours, and then reacted with melted ODA at 120-130°C for 72 hours to introduce long-chain ODA.

Planar interdigitated copper electrodes were deposited on silicon oxide substrates by conventional UV lithography and lift-off technique. The width of electrode finger and the spacing between two-neighbor electrodes were about 2  $\mu\text{m}$  and 2  $\mu\text{m}$ , respectively.

The LB films were prepared by KSV 5000 trough at room temperature. 0.7 ml chloroform solution of SWNTs (1.7 mg/ml) was dripped on the pure water subphase drop by drop to form a thin layer. After 20 minutes the organic solvent vaporized and SWNTs were left floating on the water surface. Subsequently, the floating layers were compressed by a sliding barrier at a constant speed of 4 mm/min. Then the SWNT monolayer was transferred onto silicon ( $3\times 3\text{ cm}^2$ ) or the electrodes deposited silicon oxide ( $3\times 3\text{ cm}^2$ ) substrates by vertical dipping method at fixed surface pressure of 25 mN/m, 30 mN/m and 35 mN/m, respectively. 16 layers of the SWNTs were deposited layer-by-layer with dipping directions perpendicular or

parallel to the electrodes, respectively. After deposition, UV irradiation was put on the film-coated substrates from a high pressure mercury lamp and some alkyl chains were decomposed and evaporated.

Field emission scanning electron microscopy (Sirion 200 Philips) was performed on the aligned SWNTs. I-V characteristics measurement was carried out by a semiconductor parameter analyzer Agilent model 4156C.

### 3. Results and discussion

In Fig. 1, the FTIR spectra show that the band of carboxylic groups (at  $1719\text{ cm}^{-1}$ ) is almost replaced by the band corresponding to amide C=O stretching vibration (at  $1579\text{ cm}^{-1}$ ) after chemical modification, which indicate that the long-chain ODA is introduced to SWNTs successfully.

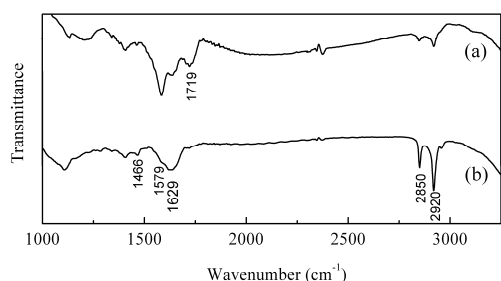


Fig. 1 FTIR spectra of SWNTs (a) before and (b) after functionalized with ODA.

In Fig. 1(b), the peaks at  $2920\text{ cm}^{-1}$  and  $2850\text{ cm}^{-1}$  are derived from the C-H stretch modes in the alkyl chain. The peak at  $1629\text{ cm}^{-1}$  is probably due to the N-H bend of the amide. And the peak at  $1466\text{ cm}^{-1}$  is from the C-H bend [22]. The scheme is shown as [23, 24]

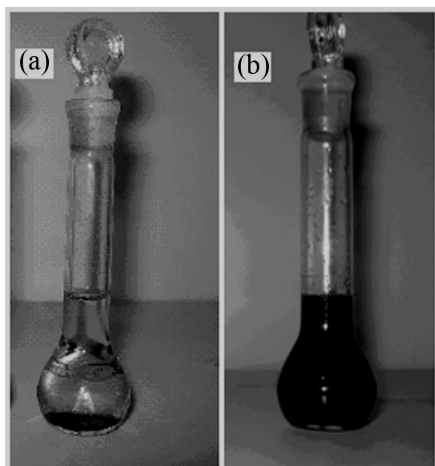
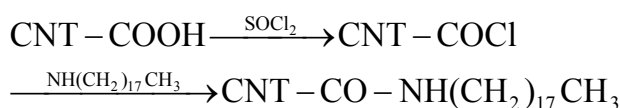


Fig. 2 (a) SWNTs in chloroform before functionalization. (b) 2.0 mg/ml SWNTs-ODA solution.

Fig. 2 shows the SWNTs dispersing in chloroform before and after functionalization, respectively. It is found that the solubility and dispersivity of SWNTs are greatly enhanced by the surface modification treatment. In Fig. 2(a), the SWNTs without chemical modification are insoluble in organic solvent and most SWNTs aggregate and precipitate in the solvent, while the functionalized SWNTs form uniform and stable suspension with solubility of 2.0 mg/ml as shown in Fig. 2(b). The dissolution of functionalized SWNTs in organic solvents is mainly associated with the long-chain ODA which is added to the SWNT ends and to the defects in the SWNT wall. In addition, the surface modification may lead to the weakening of the mutual attractive force between SWNTs, causing exfoliation of the SWNTs bundles into individual nanotubes [25], which would also contribute to the dissolution. The decorating process is very essential for successful SWNT LB film assembly, because after functionalization the tubes could not only widely spread on the air/water surface without aggregations, but also float on the subphase without sinking into the water.

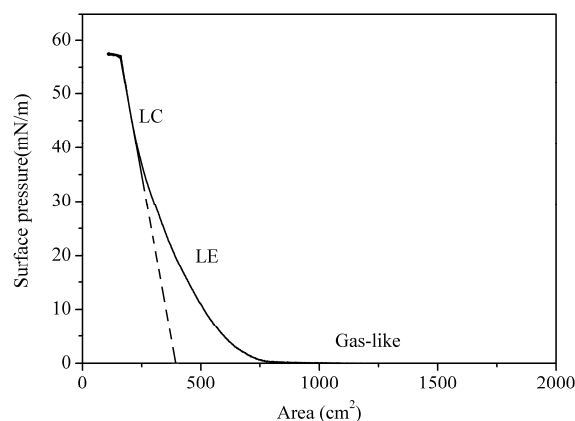


Fig. 3. Surface pressure-area isotherm of the monolayer of SWNTs on pure water surface at room temperature.

Fig. 3 recorded the surface pressure-area ( $\pi - A$ ) isotherm at room temperature. An increase of the surface pressure is displayed with the decrease of the trough area, indicating the formation of condensed SWNT monolayer. When the area roughly ranges from  $2000\text{ cm}^2$  to  $750\text{ cm}^2$ , the pressure is practically unaffected by the barrier movement. This shows that the SWNTs are largely dispersed on the water in a gas-like phase. When the pressure starts to increase from about  $750\text{ cm}^2$ , the SWNTs are still loosely arranged but in a quite packed liquid expanded (LE) phase. At an area of about  $300\text{ cm}^2$ , a further increase of the curve slope indicates the formation of a liquid condensed (LC) phase. A high collapse pressure (up to  $57\text{ mN/m}$ ) is recorded. This  $\pi - A$  isotherm indicates that the monolayer of SWNTs has good surface spreading properties. This is greatly attributed to the functionalization as the carboxylic and amide groups

introduced by the chemical treatments probably play an important role in these processes. By extrapolation to zero pressure of the curve segment relative to the LC phase, a limiting area of about  $390 \text{ cm}^2$  is obtained, which is the occupied surface area of the condensed monolayer on the water surface. The density of SWNTs is estimated to be approximately  $3.05 \times 10^{-4} \text{ mg/cm}^2$ .

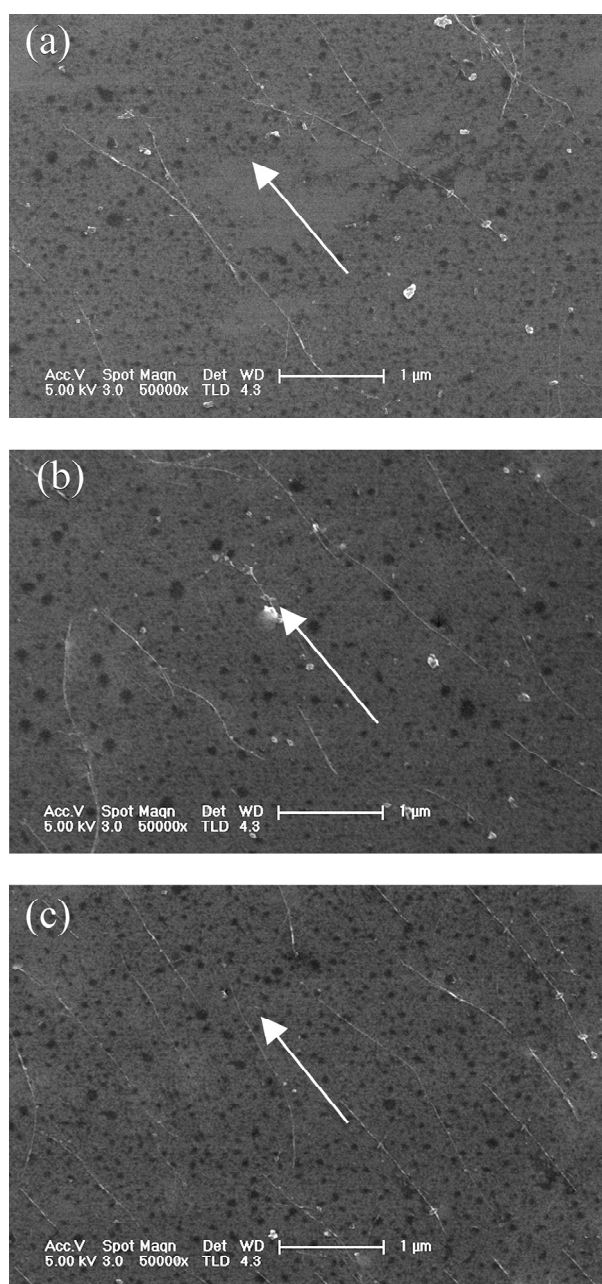


Fig.4 SEM of SWNT monolayers on silicon substrates obtained at different surface pressures: (a) 25 mN/m, (b) 30 mN/m, and (c) 35 mN/m, respectively. White arrows indicate the dipping directions.

Fig. 4 shows the SEM images of SWNT monolayers on silicon substrates dipped at surface pressures of 25 mN/m, 30 mN/m, and 35 mN/m, respectively. Large area ( $3 \times 3 \text{ cm}^2$ ) of the substrates is coated. According to the images, ordered alignment of SWNTs is achieved. The SWNTs are predominately oriented parallel and toward the dipping directions indicated by the white arrows in the SEM images. The alignment occurs because the entropy of the self-assembled structure can be maximized by minimizing the excluded volume per particle in the arrangement upon compression, such as parallel alignment of SWNTs in our system. It is found that the surface pressure has a significant influence on the alignment effect of the SWNTs. The order degree is the highest in the sample at surface pressure of 35 mN/m (Fig. 4(c)), which indicates that relatively stronger compression would benefit the alignment. Shown in Fig. 4(a), when the surface pressure is 25 mN/m, a thinner monolayer is fabricated and the average distance between the neighbouring tubes is  $\sim 2 \mu\text{m}$ . When the surface pressure increases to 30 mN/m, a denser film of SWNTs forms and the inter-particle distance decreases to  $\sim 1 \mu\text{m}$  as shown in Fig.4 (b). When the surface pressure reaches 35 mN/m, a more condensed film forms and the distance decreases to  $\sim 0.5 \mu\text{m}$  as shown in Fig. 4(c). It can be inferred that more ordered arrangement and more closely packed fashion would form under relatively stronger compression. The structure of the alignment can be controllable by the compression process. It is known that two efficient mechanisms for LB assisted alignment exist during the whole process: compression-induced arrangement and flow-induced arrangement [26]. We suggest that the former has stronger influence on the inter-particle distances, and the latter interferes with the orientation of the arrangement more efficiently.

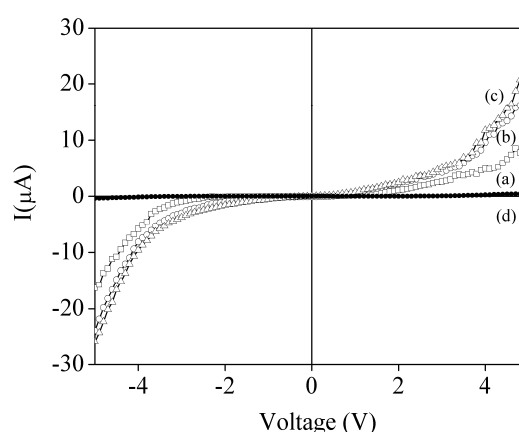


Fig. 5 Room temperature current-voltage characteristics of 16 layers with dipping direction perpendicular to the electrodes at surface pressures of (a) 25 mN/m, (b) 30 mN/m, and (c) 35 mN/m, respectively, and (d) parallel to the electrodes at surface pressures of 35 mN/m.

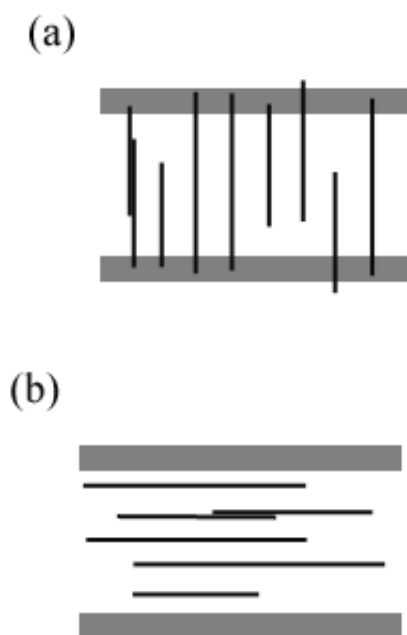


Fig. 6 The alignment of carbon nanotubes perpendicular and parallel to the electrodes, respectively.

When using LB technique, the multilayer deposited layer-by-layer is easy and efficient to be carried out. The films are homogeneous as they tend to retain a uniform and high transfer ratio ( $>0.93$ ) up to a large number of deposited layers. 16 layers of aligned SWNTs are obtained. The electrical transport characteristics of multilayer films are also studied in the experiment. Figs. 5(a) to (c) show the room temperature I-V curves of the SWNTs aligned at surface pressure of 25 mN/m, 30 mN/m, and 35 mN/m, respectively. The dipping directions are perpendicularly to the electrodes as shown in Fig. 6(a). The current transport between the electrodes displays a nonlinear dependence of applied voltage, which is due to the Schottky barrier at nanotube-metal contacts. The resistance of SWNTs aligned between electrodes is up to  $\sim 10^6$  ohm which is much larger than that of ideal ballistic SWNTs ( $\sim 10^3$  ohm), indicating that the SWNTs do not form good electrical contact with the electrodes. The reason is that the SWNTs are coupled to the electrodes by a very weak van der Waals force, as the alkyl chains attached on SWNTs contribute to the resistance which has been reported [27]. The UV irradiation would improve the contacts to some extent. The current flow increases slightly along with the increasing surface pressure. This is because at higher surface pressure, the density of the aligned nanotubes enhances, which would lead to more connections between the electrodes. This is consistent with the SEM results. Another reason is that, in the multilayers which have high density of SWNTs, more efficient electron transfer would occur between neighboring nanotubes because of the shorter tunneling barriers [28]. Fig.6 shows the alignment scheme of carbon nanotubes perpendicular and parallel to the electrodes, respectively. When the SWNTs are aligned parallel to the electrodes,

the current decreases to a very small value as shown in Fig. 5(d). This is because the alignment parallel to the electrodes greatly reduces the SWNTs connecting the electrodes (Fig. 6(b)). This is also a proof that the SWNTs have a highly ordered alignment.

#### 4. Conclusions

SWNTs were functionalized with ODA. According to the FTIR spectra, the carboxylic group band is replaced by the amide C=O stretching vibration band after modification, indicating that the long-chain ODA is introduced to the SWNTs. The functionalized SWNTs could form stable solution in chloroform solvent without aggregation at relatively high solubility (2.0 mg/ml). The  $\pi-A$  isotherm curves indicated that the chemically functionalized SWNTs have good surface spreading properties. Large-area and highly ordered SWNTs prepared at different surface pressures were observed by SEM. Multilayers of SWNT LB films were also obtained. I-V characteristics of 16 layers were investigated. When the SWNTs aligned perpendicularly to the electrodes, the curves showed a nonlinear relationship between the current and applied voltage and a current increase with increasing surface pressure. When the SWNTs were oriented parallel to the electrodes, the current was reduced to a very small value.

#### References

- [1] R. Saito, G. Dresselhaus, M. S. Dresselhaus, Physical properties of carbon nanotubes, Imperial College Press, London (1998).
- [2] X. Sun, R. Li, B. Stansfield, J. P. Dodelet, S. Désilets, Chem Phys Lett **394**, 266 (2004).
- [3] C. Dekker, Phys. Today. **52**, 22 (1999).
- [4] S. Iijima, Nature. **354**, 56 (1991).
- [5] W. A. deHeer, W. S. Bacsa, A. Châtelain, T. Gerfin, R. Humphrey-Baker, L. Forro, D. Ugarte, Science. **268**, 845 (1995).
- [6] S. Frank, P. Poncharal, Z. L. Wang and W. A. deHeer, Science. **280**, 1741 (1998).
- [7] G. Che, B. B. Lakshmi, E. R. Fisher and C. R. Martin, Nature. **393**, 346 (1998).
- [8] C. Liu, Y. Y. Fan, M. Liu, H. T. Cong, H. M. Cheng, M. S. Dresselhaus, Science. **286**, 1127 (1999).
- [9] Q. H. Wang, A. A. Setlur, J. M. Lauerhaas, J. Y. Dai, E. W. Seelig and R. P. H. Chang, Appl. Phys. Lett. **72**, 2912 (1998).
- [10] E. S. Snow, J. P. Novak, P. M. Campbell D. Park, Appl. Phys. Lett. **82**, 2145 (2003).
- [11] M. Endo, K. Takeuchi, S. Igarashi, K. Kobori, M. Shiraishi, H. W. Kroto, J. Phys. Chem. Solids. **54**, 1841-1848 (1993).
- [12] J. I. Sohn, S. Lee, Y.-H. Song, S.-Y. Choi, K.-I. Cho, K.-S. Nam, Appl. Phys. Lett. **78**, 901-903 (2001).
- [13] S. M. Bachilo, L. Balzano, J. E. Herrera, F. Pompeo, D. E. Resasco R. B. Weisman, J. Am. Chem. Soc.

- 125**, 11186-11187 (2003).
- [14] A. Thess, R. Lee, P. Nikolaev, H. Dai, P. Petit, J. Robert, C. Xu, Y. H. Lee, S. G. Kim, A. G. Rinzler, D. T. Colbert, G. E. Scuseria, D. Tománek, J. E. Fischer, R. E. Smalley, *Science*. **273**, 483 (1996).
- [15] K. Yamamoto, S. Akita, N. Y., *J. Phys. D: Appl. Phys.* **31**, L34 (1998).
- [16] M. S. Kumar, S. H. Lee, T. Y. Kim, T. H. Kim, S. M. Song, J. W. Yang, K. S. Nahm, E.-K. Suh, *Solid State Electron.* **47**, 2075 (2003).
- [17] J. E. Fischer, W. Zhou, J. Vavro, M. C. Llaguno, C. Guthy, R. Aggenmueller, *J. Appl. Phys.* **93**, 2157 (2003).
- [18] S.-K. Hwang, J. Lee, S.-H. Jeong, P.-S. Lee and K.-H. Lee, *Nanotechnology*. **16**, 850-858 (2005).
- [19] J. Gao, A. Yu, M. E. Itkis, E. Bekyarova, B. Zhao, S. Niyogi, R. C. Haddon, *J. Am. Chem. Soc.* **126**, 16698-16699 (2004).
- [20] H. Xin and A. T. Woolley, *Nano Lett.* **4**, 1481 (2004).
- [21] J. Liu, A. G. Rinzler, H. Dai and J. H. Hafner, *Science*. **280**, (1998).
- [22] M. A. Hamon, J. Chen, H. Hu, Y. Chen, M. E. Itkis, A. M. Rao, Peter C. Eklund and R. C. Haddon, *Adv Mater.* **11**, 834 (1999).
- [23] D. Tasis, N. Tagmatarchis, A. Bianco and M. Prato, *Chem. Rev.* **106**, 1105 (2006).
- [24] J. Chen, A. M. Rao and S. Lyuksyutov, *J. Phys.Chem.B.* **105**, 2525 (2001).
- [25] J. Chen, M. A. Hamon, H. Hu, Y. Chen, A. M. Rao, P. C. Eklund, R. C. Haddon, *Science*. **282**, 95 (1998).
- [26] J. Li and Y. Zhang, *Carbon*. **45**, 493-498 (2007).
- [27] C. Chen and Y. Zhang, *J. Phys. D: Appl. Phys.* **39**, 172 (2006).
- [28] Y. Yang, S. Chen, Q. Xue, A. Biris and W. Zhao, *Electrochimica Acta.* **50**, 3061 (2005).

---

\*Corresponding author: yfzhang@sjtu.edu.cn